Acta Mechanica 184, 61–76 (2006)
DOI 10.1007/s00707-006-0318-7

Acta Mechanica
Printed in Austria

# Nonlinear zigzag theory for electrothermomechanical buckling of piezoelectric composite and sandwich plates

**S. Kapuria** and **G. G. S. Achary**, New Delhi, India

Received August 31, 2005; revised December 21, 2005
Published online: April 20, 2006 

**Summary.** A coupled geometrically nonlinear efficient zigzag theory is presented for electrothermomechanical analysis of hybrid piezoelectric plates. The geometric nonlinearity is included in Von Karman sense. The thermal and potential fields are approximated as piecewise linear across sublayers. The deflection accounts for the transverse normal strain due to thermal and electric fields. The inplane displacements are considered to have layerwise variations, but are expressed in terms of only five primary displacement variables, independent of the number of layers. The coupled nonlinear equations of equilibrium and the boundary conditions are derived from a variational principle. The nonlinear theory is used to obtain the initial buckling response of symmetrically laminated hybrid plates under inplane electrothermomechanical loading. Analytical solutions for buckling of simply-supported plates under thermoelectric load are obtained for comparing the results with the available exact three-dimensional (3D) piezothermoelasticity solution. The comparison establishes that the present results are in excellent agreement with the 3D solution, when the pre-buckling transverse normal strain is neglected in the latter solution. The present results are also compared with the third order theory with the same number of displacement variables to highlight the positive effects of the layerwise terms in the displacement field approximations of the zigzag theory.

## 1 Introduction

Smart composite and sandwich plates with some sensory and actuator piezoelectric layers constitute an important element of adaptive structures in aerospace, aeronautical, automotive and other applications. Because of the high temperature environments (caused by solar radiation, aerodynamic and propulsive heating etc.) that these structures are often exposed to, study of thermal buckling and its control is essential for the design of such structures. A good amount of research has been dedicated to the study of thermal buckling behavior of composite and sandwich plates. Three-dimensional (3D) thermoelasticity solutions of buckling of elastic multilayered anisotropic, cross-ply and angle-ply composite plates have been presented for simply-supported boundary conditions [1]–[3]. The first order shear deformation theory (FSDT) with and without predictor-corrector procedures for shear correction factors [4]–[8], third order theories (TOTs) [9], [10], zigzag theory [11] and discrete layerwise theory (DLT) [12]

have been employed for thermal buckling analysis of composite and sandwich plates. Study on thermal buckling of hybrid laminated plates with surface-bonded or embedded piezoelectric layers is relatively limited in the open literature. The authors [13] have presented an exact 3D piezothermoelasticity solution for buckling of simply supported symmetrically laminated hybrid plates. They showed that (i) the pre-buckling transverse normal strain induced due to thermoelectric load, which is neglected in 2D plate theories, has significant effect on the buckling temperature, and (ii) electric boundary conditions (open circuit and closed circuit) too can significantly alter the buckling temperature, which can not be predicted by an uncoupled plate theory. Tzou and Zhou [14] have presented nonlinear classical laminate theory (CLT) without considering direct piezoelectric and pyroelectric coupling effects for deflection, buckling and dynamics of multilayered circular plates under thermal load. Ishiara and Noda [15] employed the uncoupled CLT to study thermal buckling of symmetrically laminated rectangular composite plates. Shen [16], [17] employed uncoupled refined TOT for thermal post-buckling analyses of symmetric cross-ply and antisymmetric angle-ply composite plates with piezo-actuators. Oh et al. [18] have presented an uncoupled DLT to study post-buckling and vibration response of piezolaminated plates under thermoelectric loads. The equivalent single layer (ESL) theories (e.g., CLT, FSDT, TOT) use the same global variations for the displacements across the entire laminate thickness and can not account for the zigzag nature of variation of the inplane displacements as obtained from the 3D solutions. DLTs are accurate, but suffer from an excessive number of displacement variables in proportion to the number of layers. The authors [19], [20] have presented a coupled efficient layerwise (zigzag) theory for linear static and buckling analysis of hybrid plates under electromechanical loading. This theory considers layerwise variations for the displacements, but the number of primary displacement variables is reduced to only five as in FSDT and refined TOT. Comparison of results of this theory with the exact 3D solutions for simply supported hybrid plates of highly inhomogeneous lay-ups established the high accuracy of this theory for the electromechanical response.

This work presents an efficient coupled geometrically nonlinear zigzag theory for hybrid plates under electrothermomechanical load. The nonlinear theory is used to obtain the thermal buckling response of symmetrically laminated hybrid plates. Both open and closed circuit conditions are considered. The geometric nonlinearity is included due to deflection only in the sense of Von Karman. The potential and thermal fields are approximated as piecewise linear across a number of subdivisions in the layers. The deflection field is sub-layerwise quadratic which explicitly accounts for the transverse normal strain induced by the electric and thermal fields. The inplane displacements are approximated as a combination of a global third order variation across the thickness and a layerwise linear variation. The number of primary displacement variables is reduced to five by enforcing exactly the conditions of zero transverse shear stresses at the top and bottom and their continuity at the layer interfaces. The nonlinear coupled equilibrium equations and boundary conditions are derived using a variational principle.

## 2 Thermal, potential and displacement field approximations of zigzag theory

The configuration of the hybrid plate made of $L$ perfectly bonded orthotropic laminas of total thickness $h$ is shown in Fig. 1. The piezoelectric layers bonded to the surfaces or embedded in the elastic laminate are of orthorhombic materials of class mm2 symmetry, with poling along

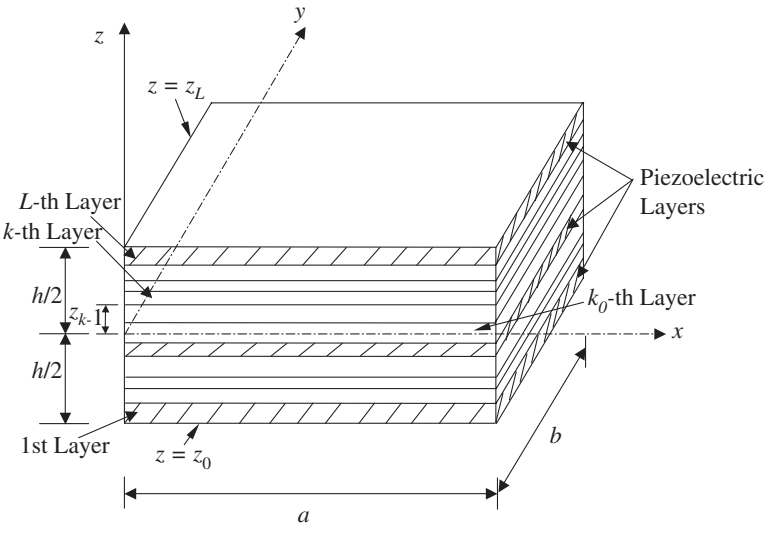


**Fig. 1.** Geometry of a hybrid plate

the $z$-direction. The reference plane $z = 0$ either passes through or is the bottom surface of the $k_0$-th layer from bottom.

Partially geometrically nonlinear strain-displacement relations in the spirit of Von Karman are employed, wherein the geometric nonlinearity due to deflection $w_0(x, y) = w(x, y, 0)$ of the midplane is included. The corresponding Lagrange strain-displacement relations and the electric field-potential relations are

$$\varepsilon_x = u_{x,x} + \frac{1}{2}w_{0,x}^2, \quad \varepsilon_y = u_{y,y} + \frac{1}{2}w_{0,y}^2, \quad \gamma_{xy} = u_{x,y} + u_{y,x} + w_{0,x}w_{0,y},$$

$$\varepsilon_z = w_{,z}, \quad \gamma_{yz} = u_{y,z} + w_{,y}, \quad \gamma_{zx} = u_{x,z} + w_{,x}, \tag{1}$$

$$E_x = -\phi_{,x}, \quad E_y = -\phi_{,y}, \quad E_z = -\phi_{,z},$$

where $u_x$, $u_y$ and $w$ denote the inplane and transverse displacements, $\phi$ denotes the electric potential, $\varepsilon_x$, $\varepsilon_y$, $\varepsilon_z$, $\gamma_{xy}$, $\gamma_{yz}$, $\gamma_{zx}$ are the strain components and $E_x$, $E_y$, $E_z$ are the electric field components. The subscript comma denotes differentiation. Considering the usual assumption of 2D plate theories, $\sigma_z \simeq 0$ [19], the 3D constitutive equations for a piezoelectric medium, relating stresses $\sigma$, $\tau$ and electric displacements $D_x, D_y, D_z$ with strains, electric field components and temperature rise $\theta$ reduce to

$$\sigma = \bar{Q}\varepsilon - \bar{e}_3^{\mathrm{T}}E_z - \bar{\beta}\theta, \quad \tau = \hat{Q}\gamma - \hat{e}E, \quad D = \hat{e}^{\mathrm{T}}\gamma + \hat{\eta}E, \quad D_z = \bar{e}_3\varepsilon + \bar{\eta}_{33}E_z + \bar{p}_3\theta, \tag{2}$$

where

$$\sigma = \begin{bmatrix} \sigma_x \\ \sigma_y \\ \tau_{xy} \end{bmatrix}, \quad \tau = \begin{bmatrix} \tau_{zx} \\ \tau_{yz} \end{bmatrix}, \quad D = \begin{bmatrix} D_x \\ D_y \end{bmatrix}, \quad \varepsilon = \begin{bmatrix} \varepsilon_x \\ \varepsilon_y \\ \gamma_{xy} \end{bmatrix}, \quad \gamma = \begin{bmatrix} \gamma_{zx} \\ \gamma_{yz} \end{bmatrix}, \quad E = \begin{bmatrix} E_x \\ E_y \end{bmatrix}, \tag{3}$$

and for general angle-ply lamina

$$\bar{Q} = \begin{bmatrix} \bar{Q}_{11} & \bar{Q}_{12} & \bar{Q}_{16} \\ \bar{Q}_{12} & \bar{Q}_{22} & Q_{16} \\ \bar{Q}_{16} & Q_{26} & \bar{Q}_{66} \end{bmatrix},\ \hat{Q} = \begin{bmatrix} \bar{Q}_{55} & \bar{Q}_{45} \\ \bar{Q}_{45} & \bar{Q}_{44} \end{bmatrix},\ \hat{e} = \begin{bmatrix} \bar{e}_{15} & \bar{e}_{14} \\ \bar{e}_{25} & \bar{e}_{24} \end{bmatrix},\ \hat{\eta} = \begin{bmatrix} \bar{\eta}_{11} & \bar{\eta}_{12} \\ \bar{\eta}_{12} & \bar{\eta}_{22} \end{bmatrix},\ \bar{\beta} = \begin{bmatrix} \bar{\beta}_1 \\ \bar{\beta}_2 \\ \bar{\beta}_6 \end{bmatrix},$$

$$\bar{e}_3 = [\,\bar{e}_{31} \quad \bar{e}_{32} \quad \bar{e}_{36}\,]. \tag{4}$$

$\bar{Q}_{ij}$, $\bar{e}_{ij}$, $\bar{\eta}_{ij}$, $\bar{\beta}_i$, $\bar{p}_3$ are the reduced elastic stiffnesses, piezoelectric stress constants, electric permittivities, stress-temperature coefficients and pyroelectric constant.

The temperature field $\theta(x,y,z)$ for the plate can be obtained by solving the heat conduction equation analytically for some geometries or by the finite element method. For the present theory, the temperature $\theta$ is assumed as piecewise linear between $n_\theta$ points $z^l_\theta$, $l = 1,2,\ldots,n_\theta$, across the thickness, and the potential $\phi$ is approximated as piecewise linear between $n_\phi$ points $z^j_\phi$, $j = 1,2,\ldots,n_\phi$, across the thickness:

$$\theta(x,y,z) = \Psi^l_\theta(z)\theta^l(x,y), \quad \phi(x,y,z) = \Psi^j_\phi(z)\phi^j(x,y), \tag{5}$$

where $\theta^l(x,y) = \theta(x,y,z^l_\theta)$, $\phi^j(x,y) = \phi(x,y,z^j_\phi)$. $\Psi^l_\theta(z)$ and $\Psi^j{}_\phi(z)$ are linear interpolation functions and summation convention is used for indices $l$ and $j$. For discretization of $\theta$, each layer can be divided into as many sublayers as required for the desired accuracy. For discretizing $\phi$, the piezoelectric layers is divided into a number of sublayers and a series of elastic layers is combined into one.

The variation of deflection $w$ is obtained by integrating the constitutive equation for $\varepsilon_z$ in which the contributions due to the thermal and electric fields are retained, i.e., $\varepsilon_z = w_{,z} \simeq -d_{33}\phi_{,z} + \alpha_3\theta \Rightarrow$

$$w(x,y,z) = w_0(x,y) - \bar{\Psi}^j_\phi(z)\phi^j(x,y) + \bar{\Psi}^l_\theta(z)\theta^l(x,y), \tag{6}$$

where $\bar{\Psi}^j{}_\phi(z) = \int_0^z d_{33}\Psi^j{}_{\phi,z}(z)dz$ is a piecewise linear function and $\bar{\Psi}^l_\theta(z) = \int_0^z \alpha_3\Psi^l_\theta(z)dz$ is a piecewise quadratic function. The inplane displacements $u_x, u_y$ for the $k$-th layer are assumed to follow a layerwise linear variation with a global third-order variation across the thickness:

$$u(x,y,z) = u_k(x,y) - zw_{0_d}(x,y) + z\psi_k(x,y) + z^2\xi(x,y) + z^3\eta(x,y), \tag{7}$$

where

$$u = \begin{bmatrix} u_x \\ u_y \end{bmatrix}, \quad w_{0_d} = \begin{bmatrix} w_{0,x} \\ w_{0,y} \end{bmatrix}, \quad u_k = \begin{bmatrix} u_{k_x} \\ u_{k_y} \end{bmatrix}, \quad \psi_k = \begin{bmatrix} \psi_{k_x} \\ \psi_{k_y} \end{bmatrix}, \quad \xi = \begin{bmatrix} \xi_x \\ \xi_y \end{bmatrix}, \quad \eta = \begin{bmatrix} \eta_x \\ \eta_y \end{bmatrix}, \tag{8}$$

$u_k$ is the translation and $\psi_k$ is related to the shear rotation of the $k$-th layer. For the mid-plane which passes through the $k_0$-th layer, denote $u_0(x,y) = u_{k_0}(x,y) = u(x,y,0)$, $\psi_0(x,y) = \psi_{k_0}(x,y)$. Using the $2(L-1)$ conditions each for the continuity of $u$ and the transverse shear stresses $\tau$ at the layer interfaces and the four shear traction-free conditions, the $(4L+4)$ variables $u_k$, $\psi_k$, $\xi$, $\eta$ in Eq. (7) are expressed in terms of only 4 variables $u_0$ and $\psi_0$ to yield

$$u(x,y,z) = u_0(x,y) - zw_{0_d}(x,y) + R^k(z)\psi_0(x,y) + R^{kj}(z)\phi^j_d(x,y) + \bar{R}^{kl}(z)\theta^l_d(x,y), \tag{9}$$

where $\phi^j_d = [\phi^j_{,x}\ \phi^j_{,y}]^{\mathrm{T}}$, $\theta^l_d = [\theta^l_{,x}\ \theta^l_{,y}]^{\mathrm{T}}$ and $R^k(z)$, $R^{kj}(z)$, $\bar{R}^{kl}(z)$ are $2\times 2$ matrices of layerwise cubic functions of $z$ whose coefficients are dependent on the material properties and the lay-ups.

## 3 Coupled nonlinear equations of equilibrium

Let the plate be subjected to normal forces $p_z^1$, $p_z^2$ per unit area on the bottom and top surfaces along the $z$-direction. $q_{j_i}$ is the the extraneous surface charge density at the interface $z = z_\phi^{j_i}$, where $\phi^{j_i}$ is prescribed. The total number of such prescribed potentials is $\bar{n}_\phi$. The variational principle for the piezoelectric medium [21] can be expressed, using the notation $\langle \ldots \rangle = \sum_{k=1}^{L} \int_{z_{k-1}^+}^{z_k^-} (\ldots)\, dz$ for integration across the thickness, as

$$\int_A [\langle \sigma_x \delta\varepsilon_x + \sigma_y \delta\varepsilon_y + \tau_{xy}\delta\gamma_{xy} + \tau_{yz}\delta\gamma_{yz} + \tau_{zx}\delta\gamma_{zx} + D_x \delta\phi_{,x} + D_y \delta\phi_{,y} + D_z \delta\phi_{,z}\rangle$$
$$- p_z^1 \delta w(x,y,z_0) - p_z^2 \delta w(x,y,z_L) + D_z(x,y,z_0)\delta\phi^1 - D_z(x,y,z_L)\delta\phi^{n_\phi} - q_{j_i}\delta\phi^{j_i}]dA$$
$$- \int_{\Gamma_L} \langle \sigma_n \delta u_n + \tau_{ns}\delta u_s + \tau_{nz}\delta w + D_n \delta\phi\rangle ds = 0, \ \forall\ \delta u_0, \delta w_0, \delta\psi_0, \delta\phi^j, \tag{10}$$

where $A$ denotes the mid-plane surface area of the plate and $\Gamma_L$ is the boundary curve of the midplane of the plate with normal $n$ and tangent $s$. The above variational equation is expressed in terms of $\delta u_0$, $\delta w_0$, $\delta\psi_0$, $\delta\phi^j$ and stress and electric displacement resultants to yield the nonlinear equilibrium equations and the boundary conditions. The stress resultants $N = [N_x N_y N_{xy}]^{\mathrm{T}}$, $M = [M_x M_y M_{xy}]^{\mathrm{T}}$, $P = [P_x P_{yx} P_{xy} P_y]^{\mathrm{T}}$, $S^j = [S^j{}_x S^j{}_{yx} S^j{}_{xy} S^j{}_y]^{\mathrm{T}}$, $Q = [Q_x Q_y]^{\mathrm{T}}$, $\bar{Q}^j = [\bar{Q}_x^j \bar{Q}_y^j]^{\mathrm{T}}$, $V = [V_x V_y]^{\mathrm{T}}$, $V_\phi^j = [V_{\phi_x}^j V_{\phi_y}^j]^{\mathrm{T}}$ and the electric displacement resultants $H^j = [H_x^j H_y^j]^{\mathrm{T}}$ and $G^j$ are defined by

$$F_1 = \begin{bmatrix} N^{\mathrm{T}} & M^{\mathrm{T}} & P^{\mathrm{T}} & S^{j\mathrm{T}} \end{bmatrix}^{\mathrm{T}} = [\langle f_3^{\mathrm{T}} \sigma\rangle], \qquad F_2 = \begin{bmatrix} Q_x & Q_y & \bar{Q}_x^j & \bar{Q}_y^j \end{bmatrix}^{\mathrm{T}} = [\langle f_4^T \tau\rangle]$$
$$V = \langle \tau\rangle, \quad V^j{}_\phi = \langle \bar{\mathbf{\Psi}}^j{}_\phi \tau\rangle, \qquad H^j = \langle \mathbf{\Psi}^j{}_\phi(z) D\rangle, \qquad G^j = \langle \mathbf{\Psi}^j{}_{\phi,z}(z) D_z\rangle, \tag{11}$$

where $f_3 = \begin{bmatrix} I_3 & zI_3 & \mathbf{\Phi}^k & \mathbf{\Phi}^{kj} \end{bmatrix}$, $f_4 = \begin{bmatrix} R_{,z}^k & R_{,z}^{kj} - \bar{\mathbf{\Psi}}^j{}_\phi(z) I_2 \end{bmatrix}$, $I_n$ being a $n \times n$ identity matrix and

$$\mathbf{\Phi}^k = \begin{bmatrix} R_{11}^k & 0 & R_{12}^k & 0 \\ 0 & R_{21}^k & 0 & R_{22}^k \\ R_{21}^k & R_{11}^k & R_{22}^k & R_{12}^k \end{bmatrix}, \quad \mathbf{\Phi}^{kj} = \begin{bmatrix} R_{11}^{kj} & 0 & R_{12}^{kj} & 0 \\ 0 & R_{21}^{kj} & 0 & R_{22}^{kj} \\ R_{21}^{kj} & R_{11}^{kj} & R_{22}^{kj} & R_{12}^{kj} \end{bmatrix}. \tag{12}$$

Using the definitions in Eq. (12), Eq. (10) yields the following coupled nonlinear field equations consisting of five equations of force equilibrium and $n_\phi$ equations for charge equilibrium:

$$N_{x,x} + N_{xy,y} = 0, \qquad N_{xy,x} + N_{y,y} = 0,$$
$$M_{x,xx} + 2M_{xy,xy} + M_{y,yy} + (N_x w_{0,x} + N_{xy} w_{0,y})_{,x} + (N_{xy} w_{0,x} + N_y w_{0,y})_{,x} + F_3 = 0,$$
$$P_{x,x} + P_{yx,y} - Q_x = 0, \qquad P_{xy,x} + P_{y,y} - Q_y = 0,$$
$$\bar{Q}_{x,x}^j + \bar{Q}_{y,y}^j - S_{x,xx}^j - S_{xy,xy}^j - S_{yx,xy}^j - S_{y,yy}^j + H_{x,x}^j + H_{y,y}^j - G^j + F^j{}_6 = 0, \quad j = 1, 2, \ldots, n_\phi, \tag{13}$$

where the mechanical load $F_3 = p_z^1 + p_z^2$ and the electrical loads $F^j{}_6 = D_z(x,y,z_L)\delta_{jn_\phi} - D_z(x,y,z_0)\delta_{j1} + q_{j_i}\delta_{jj_i}$. The five equilibrium equations in Eq. (13) correspond to the balance of linear momentum and moment of momentum for the static case. The variationally consistent boundary conditions obtained from Eq. (10) are the prescribed values of one of the factors of each of the following products:

$$u_{0_n}N_n, \quad u_{0_s}N_{ns}, \quad w_0(V_n + M_{ns,s} + N_n w_{0,n} + N_{ns}w_{0,s}), \quad w_{0,n}M_n,$$
$$\psi_{0_n}P_n, \quad \psi_{0_s}P_{ns}, \quad \phi_{,n}{}^j S_n^j, \quad \phi^j[H_n^j - V^j{}_{\phi_n} - S^j{}_{ns,s}] \tag{14}$$
$$\text{and at corners } s_i: \quad w_0(s_i)\Delta M_{ns}(s_i), \quad \phi^j(s_i)\Delta S_{ns}^j(s_i)$$

with

$$V_n = (M_{x,x} + M_{xy,y})n_x + (M_{xy,x} + M_{y,y})n_y,$$
$$V_{\phi_n}^j = (S_{x,x}^j + S_{yx,y}^j)n_x + (S_{y,y}^j + S_{xy,x}^j)n_y - \bar{Q}_x^j n_x - \bar{Q}_y^j n_y.$$

Substituting the expressions of $\sigma$, $\tau$, $D$, $D_z$ from Eq. (2) into Eq. (11) and using Eqs. (1), (5), (6) and (9) yields

$$F_1 = A\bar{\varepsilon}_1 + \beta^{j'}\phi^{j'} + A^l\theta_{dd}^l - \gamma^l\theta^l + \frac{1}{2}A^*\Phi^w w_{0_d}, \quad F_2 = \bar{A}\bar{\varepsilon}_2 + \bar{\beta}^{j'}\phi_d^{j'} + \bar{A}^l\theta_d^l,$$
$$G^j = \beta^{j\mathrm{T}}\bar{\varepsilon}_1 - E^{jj'}\phi^{j'} + \beta^{jl}\theta_{dd}^l + \gamma^{jl}\theta^l + \frac{1}{2}\beta^{jw}\Phi^w w_{0_d}, \quad H^j = \bar{\beta}^{j\mathrm{T}}\bar{\varepsilon}_2 - \bar{E}^{jj'}\phi_d^{j'} + \bar{\beta}^{jl}\theta_d^l, \tag{15}$$

where

$$\bar{\varepsilon}_1 = \big[u_{0_x,x}\ u_{0_y,y}\ u_{0_x,y} + u_{0_y,x} - w_{0,xx} - w_{0,yy}$$
$$-2w_{0,xy}\ \psi_{0_x,x}\ \psi_{0_x,y}\ \psi_{0_y,x}\ \psi_{0_y,y}\ \phi_{,xx}^j\ \phi_{,xy}^j\ \phi_{,yx}^j\ \phi_{,yy}^j\big]^{\mathrm{T}},$$
$$\bar{\varepsilon}_2 = \begin{bmatrix}\psi_{0_x} & \psi_{0_y} & \phi_{,x}^j & \phi_{,y}^j\end{bmatrix}^{\mathrm{T}}, \quad \Phi^w = \begin{bmatrix} w_{0,x} & 0 \\ 0 & w_{0,y} \\ w_{0,y} & w_{0,x}\end{bmatrix}, \quad \bar{\Phi}^{kl} = \begin{bmatrix} \bar{R}_{11}^{kl} & 0 & \bar{R}_{12}^{kl} & 0 \\ 0 & \bar{R}_{21}^{kl} & 0 & \bar{R}_{22}^{kl} \\ \bar{R}_{21}^{kl} & \bar{R}_{11}^{kl} & \bar{R}_{22}^{kl} & \bar{R}_{12}^{kl}\end{bmatrix}, \tag{16}$$

$$[A,\ A^l,\ A^*] = \langle f_3^{\mathrm{T}}(z)\bar{Q}[f_3(z),\ \bar{\Phi}^{kl}(z),\ I_3]\rangle, \quad [\bar{A},\ \bar{A}^l] = \langle f_4^{\mathrm{T}}(z)\hat{Q}[f_4(z),\ \bar{\Gamma}^{\,kl}(z)]\rangle,$$
$$\beta^{j'} = \langle f_3^{\mathrm{T}}(z)\bar{e}_3^{\mathrm{T}}\Psi_{\phi,z}^{j'}(z)\rangle, \quad \bar{\beta}^{j'} = \langle f_4^{\mathrm{T}}(z)\hat{e}\Psi_{\phi}^{\ j'}(z)\rangle, \quad E^{jj'} = \langle\bar{\eta}_{33}\Psi_{\phi,z}^{\ j}(z)\Psi_{\phi,z}^{\ j'}(z)\rangle,$$
$$\bar{E}^{jj'} = \langle\hat{\eta}\Psi_{\phi}^{\ j}(z)\Psi_{\phi}^{\ j'}(z)\rangle,$$
$$\bar{\Gamma}^{\,kl}(z) = \bar{R}_{,z}^{\ kl}(z) + \bar{\Psi}_{\theta}^{\ l}(z)I_2, \quad \gamma^{\,l} = \langle\bar{f}_3^{\mathrm{T}}(z)\bar{\beta}\Psi_{\theta}^{\ l}(z)\rangle, \quad \gamma^{jl} = \langle\hat{p}_3\Psi_{\phi,z}^{\ j}(z)\Psi_{\theta}^{\ l}(z)\rangle,$$
$$\beta^{jl} = \langle\Psi_{\phi,z}^{\ j}(z)\bar{e}_3\bar{\Phi}^{kl}(z)\rangle, \quad \bar{\beta}^{jl} = \langle\Psi_{\phi}^{\ j}(z)\hat{e}^{\mathrm{T}}\bar{\Gamma}^{\,kl}(z)\rangle, \quad \beta^{jw} = \langle\bar{e}_3\Psi_{\phi,z}^{\ j}\rangle,$$

$$A = \begin{bmatrix} A_{11} & A_{12} & \dots & A_{1,10} & A_{1,11}^{j'} & A_{1,12}^{j'} & A_{1,13}^{j'} & A_{1,14}^{j'} \\ A_{21} & A_{22} & \dots & A_{2,10} & A_{2,11}^{j'} & A_{2,12}^{j'} & A_{2,13}^{j'} & A_{2,14}^{j'} \\ \vdots & \vdots & \vdots & \vdots & \vdots & \vdots & \vdots & \vdots \\ A_{10,1} & A_{10,2} & \dots & A_{10,10} & A_{10,11}^{j'} & A_{10,12}^{j'} & A_{10,13}^{j'} & A_{10,14}^{j'} \\ A_{11,1}^{j} & A_{11,2}^{j} & \dots & A_{11,10}^{j} & A_{11,11}^{jj'} & A_{11,12}^{jj'} & A_{11,13}^{jj'} & A_{11,14}^{jj'} \\ A_{12,1}^{j} & A_{12,2}^{j} & \dots & A_{12,10}^{j} & A_{12,11}^{jj'} & A_{12,12}^{jj'} & A_{12,13}^{jj'} & A_{12,14}^{jj'} \\ A_{13,1}^{j} & A_{13,2}^{j} & \dots & A_{13,10}^{j} & A_{13,11}^{jj'} & A_{13,12}^{jj'} & A_{13,13}^{jj'} & A_{13,14}^{jj'} \\ A_{14,1}^{j} & A_{14,2}^{j} & \dots & A_{14,10}^{j} & A_{14,11}^{jj'} & A_{14,12}^{jj'} & A_{14,13}^{jj'} & A_{14,14}^{jj'} \end{bmatrix} = A^{\mathrm{T}}, \quad \beta^{j'} = \begin{bmatrix} \beta_{\ 1}^{j'} \\ \beta_{\ 2}^{j'} \\ \vdots \\ \beta_{\ 10}^{j'} \\ \beta_{\ 11}^{jj'} \\ \beta_{\ 12}^{jj'} \\ \beta_{\ 13}^{jj'} \\ \beta_{\ 14}^{jj'} \end{bmatrix},$$

$$A^l = \begin{bmatrix} A^l_{11} & A^l_{12} & A^l_{13} & A^l_{14} \\ A^l_{21} & A^l_{22} & A^l_{23} & A^l_{24} \\ \vdots & \vdots & \vdots & \\ A^l_{10,1} & A^l_{10,2} & A^l_{10,3} & A^l_{10,4} \\ A^{jl}_{11,1} & A^{jl}_{11,2} & A^{jl}_{11,3} & A^{jl}_{11,4} \\ A^{jl}_{12,1} & A^{jl}_{12,2} & A^{jl}_{12,3} & A^{jl}_{12,4} \\ A^{jl}_{13,1} & A^{jl}_{13,2} & A^{jl}_{13,3} & A^{jl}_{13,4} \\ A^{jl}_{14,1} & A^{jl}_{14,2} & A^{jl}_{14,3} & A^{jl}_{14,4} \end{bmatrix}, \quad A^* = \begin{bmatrix} A_{11} & A_{12} & A_{13} \\ A_{21} & A_{22} & A_{23} \\ \vdots & \vdots & \vdots \\ A_{10,1} & A_{10,2} & A_{10,3} \\ A^j_{11,1} & A^j_{11,2} & A^j_{11,3} \\ A^j_{12,1} & A^j_{12,2} & A^j_{12,3} \\ A^j_{13,1} & A^j_{13,2} & A^j_{13,3} \\ A^j_{14,1} & A^j_{14,2} & A^j_{14,3} \end{bmatrix}, \quad \gamma^{\,l} = \begin{bmatrix} \gamma^{\,l}_1 \\ \gamma^{\,l}_2 \\ \vdots \\ \gamma^{\,l}_{10} \\ \gamma^{\,jl}_{11} \\ \gamma^{\,jl}_{12} \\ \gamma^{\,jl}_{13} \\ \gamma^{\,jl}_{14} \end{bmatrix}, \tag{17}$$

$$\bar{A} = \begin{bmatrix} \bar{A}_{11} & \bar{A}_{12} & \bar{A}^{j'}_{13} & \bar{A}^{j'}_{14} \\ \bar{A}_{21} & \bar{A}_{22} & \bar{A}^{j'}_{23} & \bar{A}^{j'}_{24} \\ \bar{A}^{j}_{31} & \bar{A}^{j}_{32} & \bar{A}^{jj'}_{33} & \bar{A}^{jj'}_{34} \\ \bar{A}^{j}_{41} & \bar{A}^{j}_{42} & \bar{A}^{jj'}_{43} & \bar{A}^{jj'}_{44} \end{bmatrix} = \bar{A}^{\,\mathrm{T}}, \quad \bar{A}^{\,l} = \begin{bmatrix} \bar{A}^{l}_{11} & \bar{A}^{l}_{12} \\ \bar{A}^{l}_{21} & \bar{A}^{l}_{22} \\ \bar{A}^{jl}_{31} & \bar{A}^{jl}_{32} \\ \bar{A}^{jl}_{41} & \bar{A}^{jl}_{42} \end{bmatrix}, \quad \bar{\beta}^{\,j'} = \begin{bmatrix} \bar{\beta}^{j'}_{11} & \bar{\beta}^{j'}_{12} \\ \bar{\beta}^{j'}_{21} & \bar{\beta}^{j'}_{22} \\ \bar{\beta}^{jj'}_{31} & \bar{\beta}^{jj'}_{32} \\ \bar{\beta}^{jj'}_{41} & \bar{\beta}^{jj'}_{42} \end{bmatrix},$$

$$\bar{\beta}^{jl} = \begin{bmatrix} \bar{\beta}^{jl}_{11} & \bar{\beta}^{jl}_{12} \\ \bar{\beta}^{jl}_{21} & \bar{\beta}^{jl}_{22} \end{bmatrix}, \quad \bar{E}^{jj'} = \begin{bmatrix} \bar{E}^{jj'}_{11} & \bar{E}^{jj'}_{12} \\ \bar{E}^{jj'}_{21} & \bar{E}^{jj'}_{22} \end{bmatrix}, \quad \beta^{jl} = [\beta^{jl}_1\ \beta^{jl}_2\ \beta^{jl}_3\ \beta^{jl}_4], \quad \beta^{jw} = [\beta^{jw}_1\ \beta^{jw}_2\ \beta^{jw}_3].$$

Substituting Eq. (15) for the resultants into Eq. (13) yields the nonlinear electromechanically coupled equations of equilibrium in terms of the primary displacement and potential variables, $\bar{U}$:

$$L\bar{U} + L^n\bar{U} = \bar{P}, \tag{18}$$

where

$$\bar{U} = \left[u_{0_x}\, u_{0_y}\ \ w_0\ \ \psi_{0_x}\ \ \psi_{0_y}\ \ \phi^1\ \ \ldots\ \phi^{n_\phi}\right]^{\mathrm{T}}, \quad \bar{P} = \left[P_1\ \ P_2\ \ P_3\ \ P_4\ \ P_5\ \ P_6^1 \ldots P_6^{n_\phi}\right]^{\mathrm{T}}. \tag{19.1,2}$$

$L$ is a symmetric matrix of linear differential operators in $x$ and $y$, which are listed in [19]. $L^n\bar{U}$ are the nonlinear terms due to geometric nonlinearity. For cross-ply plates, considering that $\bar{Q}_{45} = 0$, $Q_{16} = \bar{Q}_{26} = 0$, $\bar{e}_{14} = \bar{e}_{25} = 0$, $\bar{\beta}_6 = 0$, $\bar{\eta}_{12} = 0$, $\bar{e}_{36} = 0$, the nonlinear terms $L^n\bar{U}$ are obtained as

$$\begin{aligned}
(L^n\bar{U})_1 &= \frac{1}{2}\,[A_{11}w^2_{0,\,x} + A_{12}w^2_{0,\,y}]_{,\,x} + [A_{33}w_{0,\,x}w_{0,\,y}]_{,y}, \\
(L^n\bar{U})_2 &= \frac{1}{2}[A_{21}w^2_{0,\,x} + A_{22}w^2_{0,\,y}]_{,\,y} + [A_{33}w_{0,\,x}w_{0,\,y}]_{,\,x}, \\
(L^n\bar{U})_3 &= N_x w_{0,xx} + N_y w_{0,yy} + 2N_{xy}w_{0,\,xy} + w_{0,\,x}(N_{x,\,x} + N_{xy,\,y}) + w_{0,\,y}(N_{xy,x} + N_{y,\,y}) \\
&\quad + \frac{1}{2}[A_{41}w^2_{0,x} + A_{42}w^2_{0,y}]_{,xx} + \frac{1}{2}[A_{51}w^2_{0,x} + A_{52}w^2_{0,y}]_{,yy} + [2A_{63}w_{0,x}w_{0,y}]_{,xy}, \\
(L^n\bar{U})_4 &= \frac{1}{2}[A_{71}w^2_{0,\,x} + A_{72}w^2_{0,\,y}]_{,\,x} + [A_{83}w_{0,\,x}w_{0,\,y}]_{,\,y}, \\
(L^n\bar{U})_5 &= [A_{93}w_{0,x}w_{0,y}]_{,x} + \frac{1}{2}[A_{10,1}w^2_{0,x} + A_{10,2}w^2_{0,y}]_{,y}, \\
(L^n\bar{U})_{5+j} &= \frac{1}{2}\beta^{jw}_1 w^2_{0,\,x} + \frac{1}{2}\beta^{jw}_2 w^2_{0,\,y} + \frac{1}{2}[A^j_{11,\,1}w^2_{0,\,x} + A^j_{11,\,2}w^2_{0,\,y}]_{,\,xx} \\
&\quad + [(A^j_{12,\,3} + A^j_{13,\,3})w_{0,\,x}w_{0,\,y}]_{,xy} + \frac{1}{2}[A^j_{14,\,1}w^2_{0,\,x} + A^j_{14,\,2}w^2_{0,\,y}]_{,\,yy}, \quad j = 1, \ldots n_\phi.
\end{aligned} \tag{20}$$

The elements of load vector $\bar{P}$ are

$$P_1 = -A^l_{11}\theta^l_{,xxx} - (A^l_{14}+A^l_{32}+A^l_{33})\theta^l_{,xyy} + \gamma^l_1\theta^l_{,x},$$

$$P_2 = -(A^l_{21}+A^l_{32}+A^l_{33})\theta^l_{,xxy} - A^l_{24}\theta^l_{,yyy} + \gamma^l_2\theta^l_{,y},$$

$$P_3 = -F_3 - A^l_{41}\theta^l_{,xxxx} - (A^l_{44}+A^l_{51}+2A^l_{62}+2A^l_{63})\theta^l_{,xxyy} - A^l_{54}\theta^l_{,yyyy} + \gamma^l_4\theta^l_{,xx} + \gamma^l_5\theta^l_{,yy},$$

$$P_4 = -A^l_{71}\theta^l_{,xxx} + (A^l_{74}+A^l_{82}+A^l_{83})\theta^l_{,xyy} + (\gamma^l_7+\bar{A}^l_{11})\theta^l_{,x}, \tag{21}$$

$$P_5 = -(A^l_{92}+A^l_{93}+A^l_{10,1})\theta^l_{,xxy} - A^l_{10,4}\theta^l_{,yyy} + (\gamma^l_{10}+\bar{A}^l_{22})\theta^l_{,y},$$

$$P^j_6 = -F^j_6 - (\bar{A}^{jl}_{31}+\bar{\beta}^{jl}_{11}-\beta^{jl}_1+\gamma^{jl}_{11})\theta^l_{,xx} - (\bar{A}^{jl}_{42}+\bar{\beta}^{jl}_{22}-\beta^{jl}_4+\gamma^{jl}_{14})\theta^l_{,yy}$$
$$+\gamma^{jl}\theta^l + A^{jl}_{11,1}\theta^l_{,xxxx} + (A^{jl}_{11,4}+A^{jl}_{12,2}+A^{jl}_{12,3}+A^{jl}_{13,2}+A^{jl}_{13,3}+A^{jl}_{14,1})\theta^l_{,xxyy} + A^{jl}_{14,4}\theta^l_{,yyyy}.$$

## 4 Buckling under uniform electrothermomechanical load

For buckling, consider a symmetrically laminated plate subjected to uniform inplane normal strains $\varepsilon^0_x$, $\varepsilon^0_y$, zero shear strain $\gamma^0_{xy}=0$, uniform temperature rise $\theta^0$ and actuation potentials independent of the $x$- and $y$-coordinates. This pre-buckling equilibrium state is denoted by superscript $(\,)^0$. For the symmetrically laminated plate under symmetrical loading about the $xy$-plane,

$$w^0_0 = 0, \quad \psi^0_x = \psi^0_y = 0. \tag{22}$$

Considering this, the plate constitutive equations (15) and equilibrium equations (13) yield

$$N^0_x = A_{11}\varepsilon^0_x + A_{12}\varepsilon^0_y + \beta^{j'}_1\phi^{0j'} - \gamma_1\theta^0, \tag{23.1}$$

$$N^0_y = A_{12}\varepsilon^0_x + A_{22}\varepsilon^0_y + \beta^{j'}_2\phi^{0j'} - \gamma_2\theta^0, \tag{23.2}$$

$$E^{ij'}\phi^{0j'} = \beta^j_1\varepsilon^0_x + \beta^j_2\varepsilon^0_y - F^{0j}_6 + \gamma^j\theta^0. \tag{23.3}$$

where $\gamma_1 = \sum_{l=1}^{n_\theta}\gamma^l_1$, $\gamma_2 = \sum_{l=1}^{n_\theta}\gamma^l_2$ and $\gamma^j = \sum_{l=1}^{n_\theta}\gamma^{jl}$. Defining $\Phi = \left[\,\phi^1\phi^2\ldots\phi^{n_\phi}\,\right]^{\mathrm{T}}$, $\Gamma = \left[\,\gamma^1\ \gamma^2\ldots\gamma^{n_\phi}\,\right]^{\mathrm{T}}$, $\beta_j = \left[\,\beta^1_j\ \beta^2_j\ldots\beta^{n_\phi}_j\,\right]^{\mathrm{T}}$ and $F_6 = \left[\,F^1_6\ F^2_6\ldots F^{n_\phi}_6\,\right]^{\mathrm{T}}$, Eq. (23.3) can be written in matrix form as

$$E\Phi^0 = \beta_1\varepsilon^0_x + \beta_2\varepsilon^0_y - F^0_6 + \Gamma\theta^0. \tag{24}$$

$\Phi^0$ is partitioned into a set of unknown output voltages $\Phi^0_s$ at $z^j_\phi$'s where $\phi$ is not prescribed and a set of known input actuation voltages $\Phi^0_a$ at the actuated surfaces. Accordingly, Eq. (24) is partitioned and arranged as

$$\begin{bmatrix} E_{ss} & E_{sa} \\ E_{as} & E_{aa} \end{bmatrix}\begin{bmatrix} \Phi^0_s \\ \Phi^0_a \end{bmatrix} = \begin{bmatrix} \beta_{1s} \\ \beta_{1a} \end{bmatrix}\varepsilon^0_x + \begin{bmatrix} \beta_{2s} \\ \beta_{2a} \end{bmatrix}\varepsilon^0_y - \begin{bmatrix} F^0_{6s} \\ F^0_{6a} \end{bmatrix} + \begin{bmatrix} \Gamma_s \\ \Gamma_a \end{bmatrix}\theta^0. \tag{25}$$

Solving Eq. (25) for $\Phi^0_s$ and substituting it into Eq. (23) yields the pre-buckling forces $N^0_x, N^0_y$ in terms of the known loading parameters:

$$
\begin{aligned}
N_x^0 &= (A_{11} + \beta_{1s}^{\mathrm{T}} E_{ss}^{-1} \beta_{1s}) \varepsilon_x^0 + (A_{12} + \beta_{1s}^{\mathrm{T}} E_{ss}^{-1} \beta_{2s}) \varepsilon_y^0 \\
&\quad + (\beta_{1a}^{\mathrm{T}} - \beta_{1s}^{\mathrm{T}} E_{ss}^{-1} E_{sa}) \Phi_a^0 - \beta_{1s}^{\mathrm{T}} E_{ss}^{-1} F_{6s}^0 - (\gamma_1 - \beta_{1s}^{\mathrm{T}} E_{ss}^{-1} \Gamma_s) \theta^0, \\
N_y^0 &= (A_{12} + \beta_{2s}^{\mathrm{T}} E_{ss}^{-1} \beta_{1s}) \varepsilon_x^0 + (A_{22} + \beta_{2s}^{\mathrm{T}} E_{ss}^{-1} \beta_{2s}) \varepsilon_y^0 \\
&\quad + (\beta_{2a}^{\mathrm{T}} - \beta_{2s}^{\mathrm{T}} E_{ss}^{-1} E_{sa}) \Phi_a^0 - \beta_{2s}^{\mathrm{T}} E_{ss}^{-1} F_{6s}^0 - (\gamma_2 - \beta_{2s}^{\mathrm{T}} E_{ss}^{-1} \Gamma_s) \theta^0.
\end{aligned} \tag{26}
$$

Let the solution for just after buckling be denoted by $\hat{(\,)}$ on the entities. The size of the buckling mode $\epsilon \bar{U}$ is described by an arbitrary small parameter $\epsilon$. Thus, $\hat{U} = \bar{U}^0 + \epsilon \bar{U}$ with $\bar{U}$ given by Eq. (19.1). Substituting this solution into Eqs. (18), using Eq. (22) and considering upto first order terms in $\epsilon$ yield the following stability equations for $\bar{U}$:

$$
L\bar{U} + \begin{bmatrix} 0 & 0 & (N_x^0 w_{0,\,xx} + N_y^0 w_{0,\,yy}) & 0 & 0 & 0 \end{bmatrix}^{\mathrm{T}} = \bar{P} = \begin{bmatrix} 0 & 0 & 0 & 0 & 0 & \bar{F}_6^{\,j} \end{bmatrix}^{\mathrm{T}}. \tag{27}
$$

For a set of zero incremental potential at the actuator locations, zero incremental electric displacement at the unknown potential locations and zero incremental temperature, the incremental load $\hat{F}_6^j$ is zero for index $j$ corresponding to such surfaces.

To assess the accuracy of the theory, by comparison with the available 3D piezothermoelasticity solution [13], the analytical Navier solution of Eq. (27) for buckling is obtained for simply-supported rectangular plates of sides $a$ and $b$ along the axes $x$ and $y$ for the boundary conditions

$$
\begin{aligned}
&\text{at } x = 0, a: \quad N_x, u_{0_y}, w_0, \psi_{0_y}, M_x, P_x, \phi^j, S_x^j = 0, \\
&\text{at } y = 0, b: \quad N_y, u_{0_x}, w_0, \psi_{0_x}, M_y, P_y, \phi^j, S_y^j = 0,
\end{aligned} \tag{28}
$$

for $j = 1, \ldots, n_\phi$. The solution for the $(m, n)$th spatial mode of buckling is taken as:

$$
\begin{bmatrix} w_0 & \phi^j \\ u_{0_x} & \psi_{0_x} \\ u_{0_y} & \psi_{0_y} \end{bmatrix} = \begin{bmatrix} [(w_0 \quad \phi^j)_{mn}] \sin(\bar{m}x) \sin(\bar{n}y) \\ [(u_{0_x} \quad \psi_{0_x})_{mn}] \cos(\bar{m}x) \sin(\bar{n}y) \\ [(u_{0_y} \quad \psi_{0_y})_{mn}] \sin(\bar{m}x) \cos(\bar{n}y) \end{bmatrix} \tag{29}
$$

with $\bar{m} = m\pi/a$, $\bar{n} = n\pi/b$. Substituting these into Eq. (27) yields

$$
(K - K_G)\bar{U}^{mn} = \bar{P}^{mn}, \tag{30}
$$

where $K_G$ is the geometric stiffness matrix with the only non-zero element $K_G(3,3) = -\bar{m}^2 N_x^0 - \bar{n}^2 N_y^0$. $K$ is the symmetric stiffness matrix. Partitioning electric potentials $\Phi$ into the unknown and known parts $\Phi_s$ and $\Phi_a$, Eq. (30) can be written for $\tilde{U}^{mn} = \begin{bmatrix} u_{0_{xmn}} & u_{0_{ymn}} & w_{0mn} & \psi_{0_{xmn}} & \psi_{0_{ymn}} & \Phi_s^{mn} \end{bmatrix}^{\mathrm{T}}$ as

$$
(\tilde{K} - \tilde{K}_G)\tilde{U}^{mn} = (\tilde{K} - \lambda K_G^*)\tilde{U}^{mn} = 0. \tag{31}
$$

The above equation represents a generalized eigenvalue problem and the eigenvalue $\lambda$ is the buckling load factor. The eigenvalues and eigenvectors are obtained by a QR algorithm after reducing to Heissenberg form.

## 5 Assessment of the theory for thermal buckling

For numerical evaluation of the new theory for thermal buckling response, hybrid plates of three different laminate configurations (a), (b) and (c) are considered. The stacking order is mentioned from the bottom. The elastic substrate of plate (a) has five plies of equal thickness

$0.16h$ of materials $2/1/3/1/2$ with orientations of the principal material axis 1 as $[90°/0°/0°/0°/90°]$. It is a good test case for assessing a 2D theory since the plies have highly inhomogeneous stiffness in tension and shear. The substrate of plate (b) is a graphite-epoxy composite laminate of material 4 with four layers of equal thickness $0.2h$ with lay-up $[0°/90°/90°/0°]$. The substrate of plate (c) is a five-layer sandwich having graphite-epoxy faces $[0°/90°]$ and a soft core with thicknesses $0.04h/0.04h/0.64h/0.04h/0.04h$. All the plates have two PZT-5A layers, each of thickness $0.1h$, bonded to their elastic substrate on its top and bottom surfaces. The PZT-5A layers have poling in $+z$-direction. The top and the bottom of the substrate are grounded. The material properties are selected as [13]: $[(Y_1, Y_2, Y_3, G_{12}, G_{23}, G_{31}), \nu_{12}, \nu_{13}, \nu_{23}, (\alpha_1, \alpha_2, \alpha_3)] =$

Material 1: $[(6.9, 6.9, 6.9, 1.38, 1.38, 1.38)\,\text{GPa}, 0.25, 0.25, 0.25, (35.6, 35.6, 35.6) \times 10^{-6}\,\text{K}^{-1}]$,
Material 2: $[(224.25, 6.9, 6.9, 56.58, 1.38, 56.58)\,\text{GPa}, 0.25, 0.25, 0.25, (0.25, 35.6, 35.6) \times 10^{-6}\,\text{K}^{-1}]$,
Material 3: $[(172.5, 6.9, 6.9, 3.45, 1.38, 3.45)\,\text{GPa}, 0.25, 0.25, 0.25, (0.57, 35.6, 35.6) \times 10^{-6}\,\text{K}^{-1}]$,
Material 4: $[(181, 10.3, 10.3, 7.17, 2.87, 7.17)\,\text{GPa}, 0.28, 0.28, 0.33, 0.02, 22.5, 22.5) \times 10^{-6}\,\text{K}^{-1}]$,
Face: $[(131.1, 6.9, 6.9, 3.588, 2.3322, 3.588)\ \text{GPa}, 0.32, 0.32, 0.49, (0.0225, 22.5, 22.5) \times 10^{-6}\,\text{K}^{-1}]$,
Core: $[(0.2208, 0.2001, 2760, 16.56, 455.4, 545.1)\ \text{MPa}, 0.99, 3 \times 10^{-5}, 3 \times 10^{-5}, (30.6, 30.6, 30.6) \times 10^{-6}\,\text{K}^{-1}]$,
PZT-5A: $[(61.0, 61.0, 53.2, 22.6, 21.1, 21.1)\text{GPa}, 0.35, 0.38, 0.38, (1.5, 1.5, 2.0) \times 10^{-6}\ \text{K}^{-1}]$, and

$[(d_{31}, d_{32}, d_{33}, d_{15}, d_{24}), \quad (\eta_{11}, \eta_{22}, \eta_{33}), \quad p_3] = [(-171, -171, 374, 584, 584) \times 10^{-12}\text{m/V}, (1.53, 1.53, 1.5) \times 10^{-8}\text{F/m}, 0.0007\text{Cm}^{-2}\ \text{K}^{-1}]$, where $Y_i$, $G_{ij}$, $\nu_{ij}$, $\alpha_i$, $d_{ij}$, $\eta_{ij}$ and $p_3$ denote Young's moduli, shear moduli, Poisson's ratios, coefficients of linear expansion, piezoelectric strain constants, electric permittivities and pyroelectric constant, respectively.

The pre-buckling thermal load cases consist of a uniform temperature rise $\theta^0$ of the plates with the top and bottom surfaces under (1) closed circuit condition with $\phi^1 = \phi^{n_\phi} = 0$, and (2) open circuit condition with $D_z(z_0) = D_z(z_L) = 0$. In the present problem, the open circuit condition induces a uniform sensory potential on the surfaces, as can be seen from Eq. (19). This corresponds to the piezoelectric layers being electroded at the surfaces, resulting in equipotential areas. The ends of the plates are immovable, i.e. $\varepsilon_x^0 = \varepsilon_y^0 = 0$. The critical value of $\theta^0$ for buckling is defined as $\theta_{\text{cr}}$. The results are non-dimensionalized with $S = a/h$:

$$\bar{\theta}_{\text{cr}} = \alpha_0 \theta_{\text{cr}} S^2, \quad \bar{\phi}_{\text{cr}} = \phi_{\text{cr}} d_0 S^3/a, \quad (\bar{u}, \bar{v}, \bar{w}) = (Su, Sv, w)/\max(w),$$

$$(\bar{\sigma}_x, \bar{\sigma}_y) = (\sigma_x, \sigma_y) S^2 h/Y_0 \max(w), \quad (\bar{\tau}_{zx}, \bar{\tau}_{yz}) = (\tau_{zx}, \tau_{yz}) S^3 h/Y_0 \max(w),$$

where $\max(w)$ denotes the largest value of $w$ through the thickness, $d_0 = 374 \times 10^{-12}\ \text{CN}^{-1}$, $\alpha_0 = 22.5 \times 10^{-6}\ \text{K}^{-1}$, and $Y_0 = 6.9$ GPa for laminates (a) and (c) and 10.3 GPa for laminate (b).

**Table 1.** 3D results for $\bar{\theta}_{\text{cr}}$ and $\bar{\theta}^*_{\text{cr}}$ and % errors for ZIGT and TOT with respect to 3D results for hybrid plates ($S = 20$, $b/a = 1$)

| Case | Plate | Exact | | % error in ZIGT | | % error in TOT | |
|---|---|---|---|---|---|---|---|
| | | $\bar{\theta}_{\text{cr}}$ | $\bar{\theta}^*_{\text{cr}}$ | $\bar{\theta}_{\text{cr}}$ | $\bar{\theta}^*_{\text{cr}}$ | $\bar{\theta}_{\text{cr}}$ | $\bar{\theta}^*_{\text{cr}}$ |
| 1 | (a) | 12.209 | 10.785 | −11.44 | 0.25 | 2.82 | 16.40 |
| | (b) | 15.844 | 14.410 | −8.75 | 0.33 | 7.48 | 1.72 |
| | (c) | 32.692 | 27.099 | −16.85 | 0.31 | 6.84 | 12.39 |
| 2 | (a) | 7.7703 | 7.1767 | −7.30 | 0.36 | 8.06 | 17.00 |
| | (b) | 8.7090 | 8.2679 | −4.61 | 0.48 | 3.21 | 1.95 |
| | (c) | 7.8339 | 7.4735 | −4.28 | 0.34 | 8.50 | 13.74 |

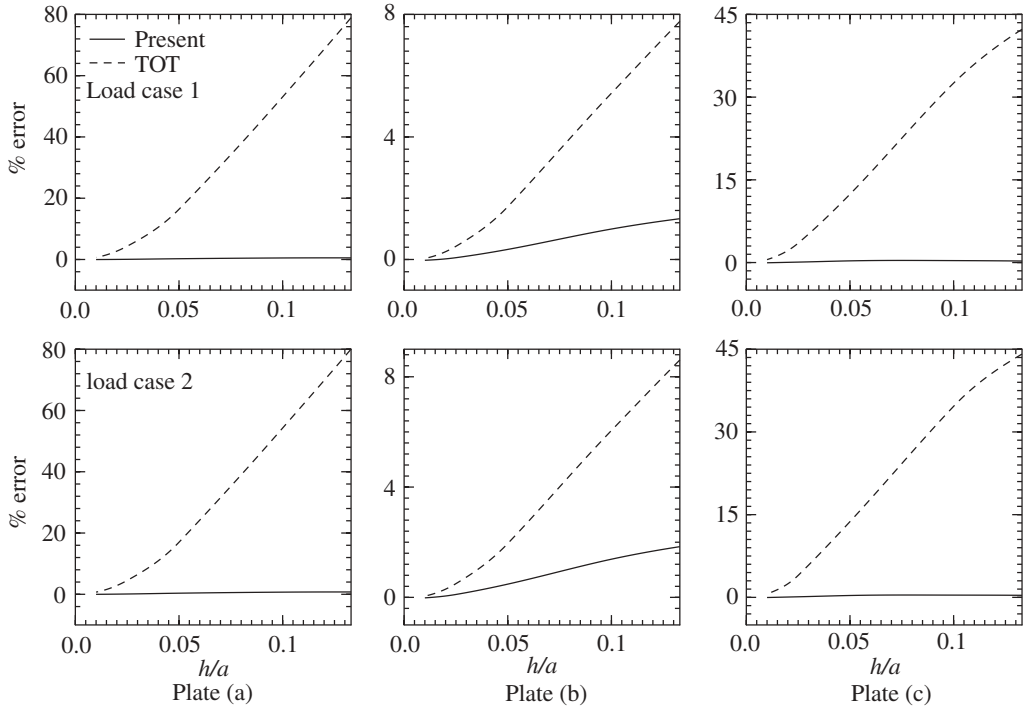


**Fig. 2.** Percentage error of buckling temperature for square hybrid plates (a), (b) and (c) under load cases 1 and 2

**Table 2.** 3D results for $\bar{\theta}^*_{\rm cr}$ of square hybrid plates (a), (b) and (c) under load cases 1 and 2

| $S$ | Plate (a) | | Plate (b) | | Plate (c) | |
|---|---|---|---|---|---|---|
| | case 1 | case 2 | case 1 | case 2 | case 1 | case 2 |
| 7.5 | 5.1220 | 3.3231 | 9.9003 | 5.5373 | 11.029 | 2.8582 |
| 10 | 6.9207 | 4.5274 | 11.721 | 6.6242 | 15.706 | 4.1436 |
| 20 | 10.785 | 7.1767 | 14.41 | 8.2679 | 27.099 | 7.4735 |
| 40 | 12.632 | 8.4744 | 15.324 | 8.8381 | 33.29 | 9.4107 |
| 100 | 13.278 | 8.9337 | 15.604 | 9.0143 | 35.59 | 10.155 |

The accuracy of the present theory for thermal buckling response is established by direct comparison with the exact 3D piezothermoelasticity solution [13] for simply-supported cross-ply symmetrically laminated hybrid plates. Since TOT uses the same global third order variation for the displacement field across the thickness, without the layerwise terms, and has the same number of displacement variables as the present theory (ZIGT), present results are also compared with the coupled TOT [22] extended for the buckling case. This comparison will establish the effect of the layerwise terms for the displacements incorporated in the ZIGT. In these nonlinear 2D plate theories, the governing equations of equilibrium do not incorporate the pre-buckling transverse normal strain $\varepsilon^0_z$. Therefore, buckling temperatures for the exact 3D solution have been obtained without and with the neglect of $\varepsilon^0_z$, which are denoted as $\bar{\theta}_{\rm cr}$ and $\bar{\theta}^*_{\rm cr}$, respectively. These results and the errors of the present theory and TOT are given in Table 1 for square hybrid plates (a), (b) and (c) with $S = 20$ for both load cases. For all plates with $b/a = 1$, the critical buckling mode corresponds to $(m, n) = (1, 1)$. It is observed that, indeed,

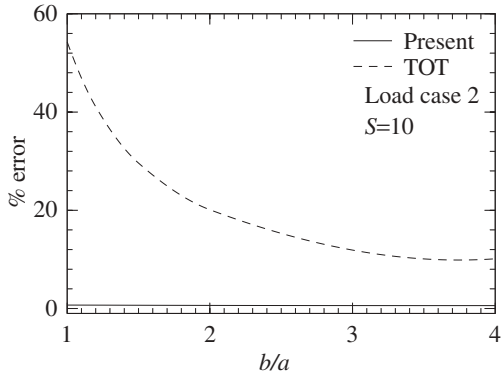


**Fig. 3.** Variation of percentage error of buckling temperature with ratio $b/a$ for plate (a)

**Table 3.** 3D results for $\bar{\theta}^*_{\rm cr}$ of plate (a) for different $b/a$ ratios (load case 2, $S = 10$)

| $b/a$ | 1.0 | 1.2 | 1.5 | 2.0 | 4.0 |
|---|---|---|---|---|---|
| $\bar{\theta}^*_{\rm cr}$ | 4.52742 | 3.89978 | 3.27611 | 2.69948 | 2.04495 |

$\varepsilon^0_z$ has a very significant effect on the buckling temperature. It is also found that the error due to neglecting $\varepsilon^0_z$ and that due to the displacement field approximations in the 2D theories are of opposite signs in many cases. Therefore, in order to ascertain the error due to displacement approximations across the laminate thickness in the 2D theories, the subsequent 3D results are obtained without considering $\varepsilon^0_z$.

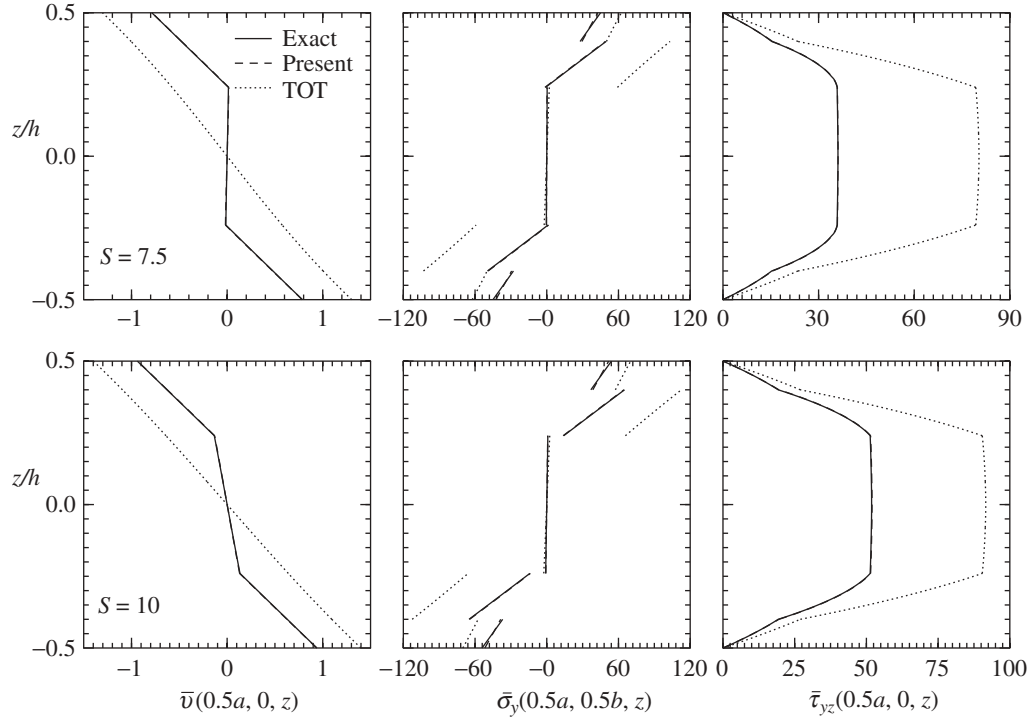


**Fig. 4.** Distributions of $\bar{v}$, $\bar{\sigma}_y$, $\bar{\tau}_{yz}$ for thermal buckling mode of square hybrid plate (a) under load case 2

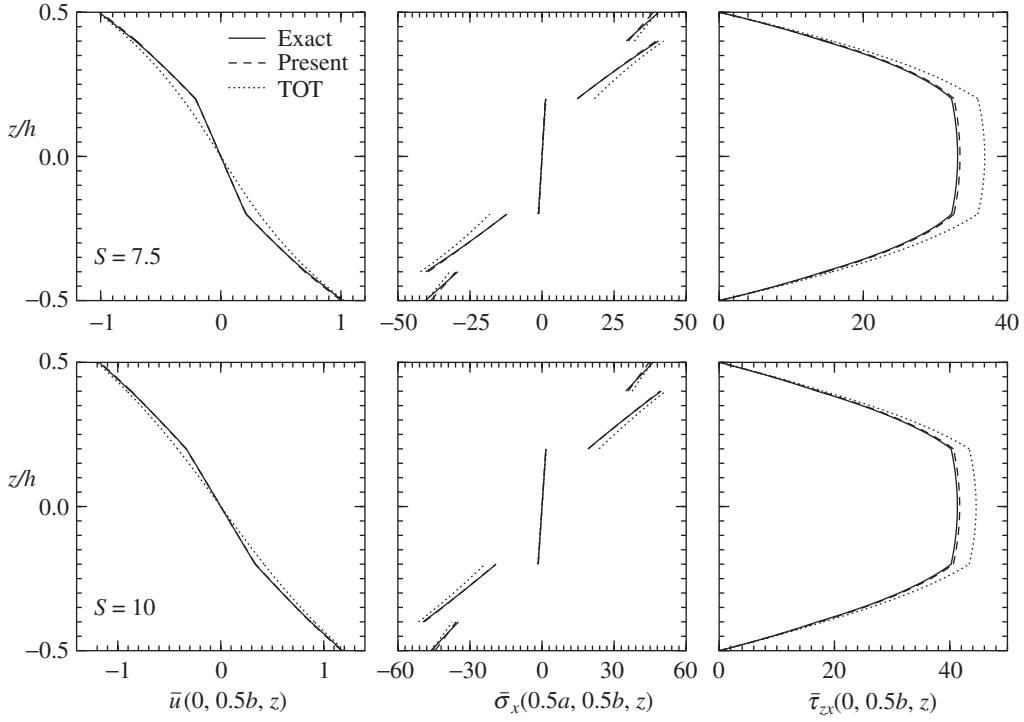


**Fig. 5.** Distributions of $\bar{u}$, $\bar{\sigma}_x$, $\bar{\tau}_{zx}$ for thermal buckling mode of square hybrid plate (b) under load case 2

The variation of the percentage error of buckling temperatures with respect to the 3D results $\bar{\theta}^*_{\rm cr}$ with the thickness parameter $h/a$ is presented in Fig. 2 for square hybrid plates (a), (b) and (c) for load cases 1 and 2. For reference, the 3D results $\bar{\theta}^*_{\rm cr}$ for span-to-thickness ratios $S = a/h = 7.5,\ 10,\ 20,\ 40,\ 100$ are listed in Table 2. It is revealed that though the buckling temperatures of plates under closed and open circuit conditions are considerably different, the errors in the 2D theories in the two cases differ only marginally. The error is generally little higher for the open circuit condition than for the closed one. The maximum error in the ZIGT for the buckling temperature for thick plates with $S = 7.5$ is 1.8%, whereas the error in TOT is 80.0, 8.6 and 44.1% for plates (a), (b) and (c), respectively. Even for thin plates with $S = 20$, the error in TOT for $\bar{\theta}^*_{\rm cr}$ is as high as 17.0% and 13.7% for plates (a) and (c). The extent of error in TOT results for plate (a) confirms that this plate indeed offers a good test case for assessing the accuracy of 2D theories for thermal buckling. The present theory successfully passes this test. As is well known, equivalent single layer theories like TOT yield highly inaccurate results for sandwich plates, whereas ZIGT yields excellent results for these plates too.

The variations of the percentage error in ZIGT and TOT for the buckling temperature with the side ratio $(b/a)$ are shown in Fig. 3 for plate (a) with $S = 10$ under load case 2. For reference, the 3D results of $\bar{\theta}^*_{\rm cr}$ of plate (a) with $S = 10$ for $b/a = 1.0,\ 1.2,\ 1.5,\ 2.0,\ 4.0$ are listed in Table 3. It is revealed that whereas the error in ZIGT remains low with little change, the error in TOT reduces with the increase in $b/a$.

The through-the-thickness distributions of predominant modal inplane displacements $\bar{u}/\bar{v}$, normal stresses $\bar{\sigma}_x/\bar{\sigma}_y$ and transverse shear stresses $\bar{\tau}_{zx}/\bar{\tau}_{yz}$ for the thermal buckling mode at $(x, y)$ locations where they are maximum are compared in Figs. 4–6 for square hybrid plates (a), (b) and (c) for load case 2 for $S = 7.5$ and 10. It is observed that the present distributions are in excellent agreement with the exact modal distributions for all plates even for the thick

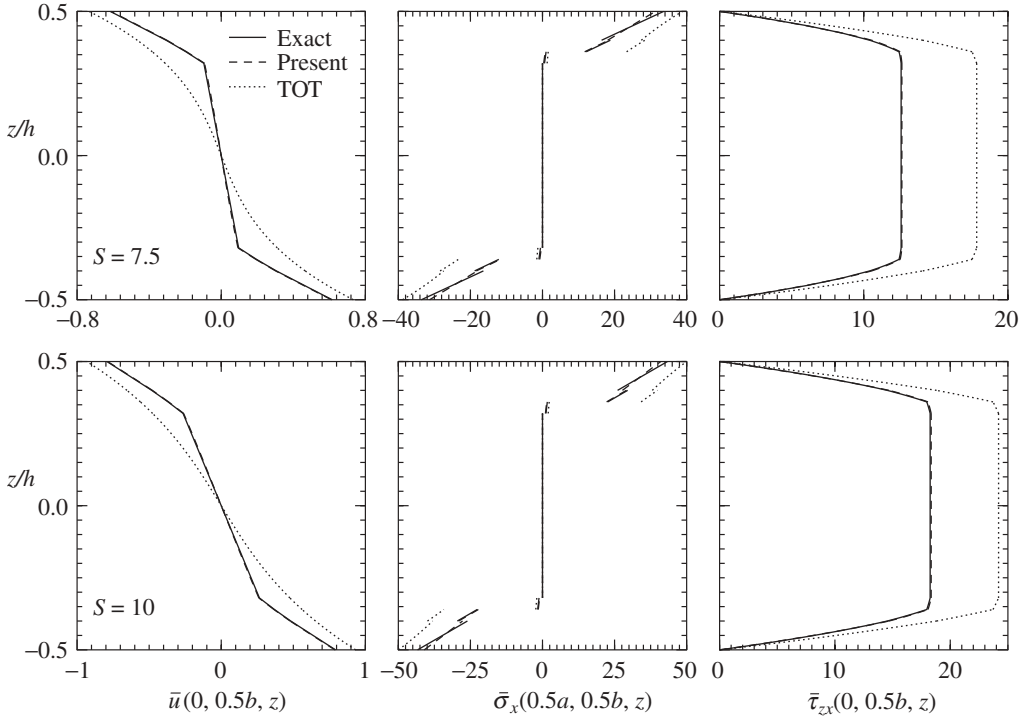


**Fig. 6.** Distributions of $\bar{u}$, $\bar{\sigma}_x$, $\bar{\tau}_{zx}$ for thermal buckling mode of square hybrid plate (c) under load case 2

ones with $S = 7.5$. In contrast, the distributions obtained from TOT have large error even for $S = 10$. The present theory is able to accurately capture the layerwise zigzag distribution of the modal inplane displacements obtained from the 3D solution, but the global distribution of the inplane displacements used in TOT is unable to capture it. This explains why ZIGT yields accurate results and TOT does not. The presented results cover a wide variety of possible cases as is evident from the qualitative distinct nature of the through-the-thickness distributions of the modal entities for the three plates.

The effect of the ratio $b/a$ on the accuracy of the through-the-thickness distributions is illustrated in Fig. 7 by plotting the distributions for two values of $b/a = 1.5$ and $b/a = 4$ for plate (a) with $S = 10$. It is seen that whereas ZIGT yields accurate distributions for all ratios $b/a$, the error in the TOT reduces with the increase in $b/a$.

## 6 Conclusions

A geometrically nonlinear electromechanically coupled zigzag theory is developed for hybrid piezoelectric plates under electrothermomechanical loading. The theory considers layerwise distribution of the inplane displacements across the thickness and accounts for the transverse normal strain caused by the thermal and potential fields, but the displacement field is expressed in terms of only five displacement variables as in TOT. The nonlinear theory is used to obtain the initial thermal buckling response of symmetrically laminated plates. The accuracy of the theory is established directly by comparison with the exact 3D piezothermoelasticity solution for a simply supported highly inhomogeneous hybrid test plate, a composite plate and a

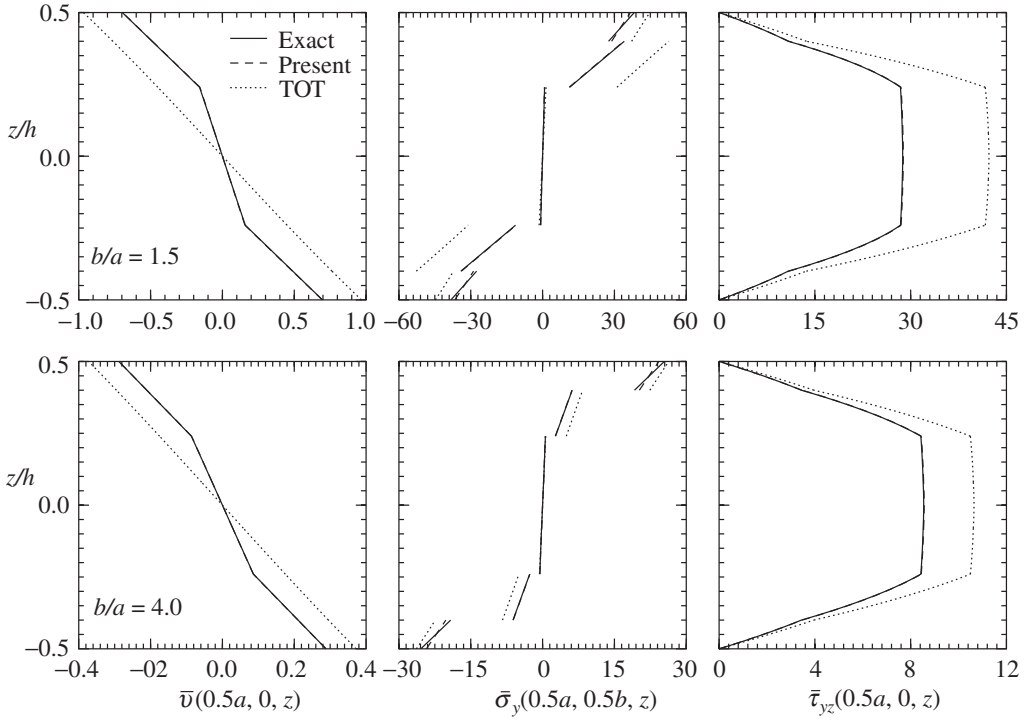


**Fig. 7.** Effect of $b/a$ on distributions of $\bar{v}$, $\bar{\sigma}_y$, $\bar{\tau}_{yz}$ for thermal buckling mode of hybrid plate (a) under load case 2

sandwich plate with the piezo-surfaces under closed and open circuit conditions. The buckling temperatures predicted by the present theory are found to be in excellent agreement with the 3D solution which neglects the pre-buckling transverse normal strain. In contrast, TOT results may have significant errors even for thin plates with $S = 20$. The present results are superior, since this theory can accurately predict the zigzag distributions of inplane displacements as obtained from 3D exact solutions. The present theory is applicable for hybrid sandwich plates too, for which TOT yields poor results.

## Acknowledgements

This work has been supported by Department of Science and Technology, Government of India, through a financial grant in SERC scheme.

## References

[1] Noor, A. K., Burton, W. S.: Three-dimensional solutions for thermal buckling of multilayered anisotropic plates. ASCE J. Engng. Mech. **118**(4), 683–701 (1992).
[2] Noor, A. K., Burton, W. S.: Three-dimensional solutions for the free vibrations and buckling of thermally stressed multilayered angle-ply composite plates. ASME J. Appl. Mech. **59**, 868–877 (1992).
[3] Noor, A. K., Burton, W. S.: Three-dimensional solutions for thermal buckling and sensitivity derivatives of temperature-sensitive multilayered angle-ply plates. ASME J. Appl. Mech. **59**, 848–855 (1992).

[4] Noor, A. K., Burton, W. S.: Predictor-corrector procedures for thermal buckling analysis of multilayered composite plates. Comput. Struct. **40**, 1071–1084 (1991).
[5] Noor, A. K., Peters, J. M.: Thermomechanical buckling of multilayered composite plates. ASCE J. Engng. Mech. **118**, 351–366 (1992).
[6] Huang, N. N., Tauchert, R. R.: Thermal buckling of clamped symmetric laminated plates. Thin-Walled Struct. **13**, 259–273 (1992).
[7] Prabhu, M. R., Dhanaraj, R.: Thermal buckling of laminated composite plates. Comput. Struct. **53**, 1193–1120 (1994).
[8] Ge, Y. S., Yuan W. X., Dawe, D. J.: Thermomechanical buckling of rectangular, shear deformable, composite laminated plates. Struct. Engng. and Mech. **13**, 411–428 (2002).
[9] Kant, T., Babu, C. S.: Thermal buckling analysis of skew fibre-reinforced composite and sandwich: plates using shear deformable finite element models. Compos. Struct. **49**, 77–85 (2000).
[10] Babu, C. S., Kant, T.: Refined higher order finite element models for thermal buckling of laminated composite and sandwich plates. J. Thermal Stress. **23**, 111–130 (2000).
[11] Shu, X., Sun, L.: Thermomechanical buckling of laminated composite plates with higher-order transverse shear deformation. Comput. Struct. **53**, 1–7 (1994).
[12] Shiau, L. C., Kuo, S. Y.: Thermal buckling of composite sandwich plates. Mechanics Based Design of Structures and Machines **32**, 57–72 (2004).
[13] Kapuria, S., Achary, G. G. S.: Exact 3D Piezothermoelasticity solution for buckling of hybrid cross-ply plates using state space approach. ZAMM **170**, 25–46 (2004).
[14] Tzou, H. S., Zhou, Y. H.: Nonlinear piezothermoelasticity and multi-field actuations, Part 2: control of nonlinear deflection, buckling and dynamics. ASME J. Vib. Accous. **119**, 382–389 (1997).
[15] Ishihara, M., Noda, N.: Nonlinear dynamic behavior of a piezothermoelastic laminated plate with anisotropic material properties Source. Acta Mech. **166**, 103–118 (2003).
[16] Shen, H. S.: Thermal postbuckling of shear deformable laminated plates with piezoelectric actuators under complex loading conditions. Int. J. Solids Struct. **38**, 7703–7721 (2001).
[17] Shen, H. S.: Thermal postbuckling of shear deformable laminated plates with piezoelectric actuators. Compos. Sci. and Tech. **61**, 1931–1943 (2001).
[18] Oh, I. K., Han, J. H., Lee, I.: Postbuckling and vibration characteristics of piezolaminated composite plate subject to thermo-piezoelectric loads. J. Sound Vibr. **233**, 19–40 (2000).
[19] Kapuria, S.: A coupled zigzag third order theory for hybrid cross-ply plates. ASME J. Appl. Mech. **71**, 604–614 (2004).
[20] Kapuria, S., Achary, G. G. S.: Nonlinear coupled zigzag theory for buckling of hybrid piezoelectric plates. Compos. Struct. (accepted for publication).
[21] Tiersten, H. F.: Linear Piezoelectric Plate Vibrations, pp. 25–37, 54, 55. New York: Plenum 1969.
[22] Kapuria S., Achary, G. G. S.: A coupled consistent third order theory for hybrid piezoelectric plates. Compos. Struct. **70**, 120–133 (2005).

**Authors' addresses:** S. Kapuria, Applied Mechanics Department, I.I.T. Delhi, Hauz Khas, New Delhi 110016, India (E-mail: kapuria@am.iitd.ac.in); G. G. S. Achary, ETD Department, Engineers India Limited, Bhikaji Cama Place, New Delhi 110066, India